Electronic Supplementary Material (ESI) for New Journal of Chemistry.
This journal is © The Royal Society of Chemistry and the Centre National de la Recherche Scientifique 2021

Unveiling the Effects of Substituents on the Packing Motif and the Carrier Transport of Dinaphtho-Thieno-Thiophene (DNTT)-based Material

Pan-Pan Lin[a], Gui-Ya Qin[a], Jing-Fu Guo[b], Bo-Hua Zhang[a], Hui-Yuan Li[a], Lu-Yi Zou [a], Ai-Min Ren[a]*

a Laboratory of Theoretical and Computational Chemistry, Institute of Theoretical Chemistry, Jilin University, Changchun, 130023, China

b: School of Physics, Northeast Normal University, Changchun 130024, P.R. China

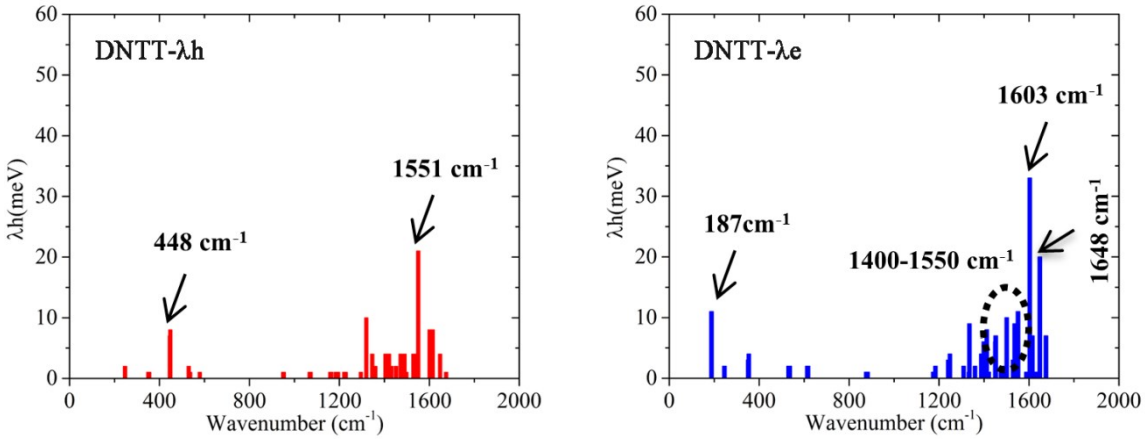

Fig. S1 The normal mode contributions to hole and electron reorganization energies for DNTT.

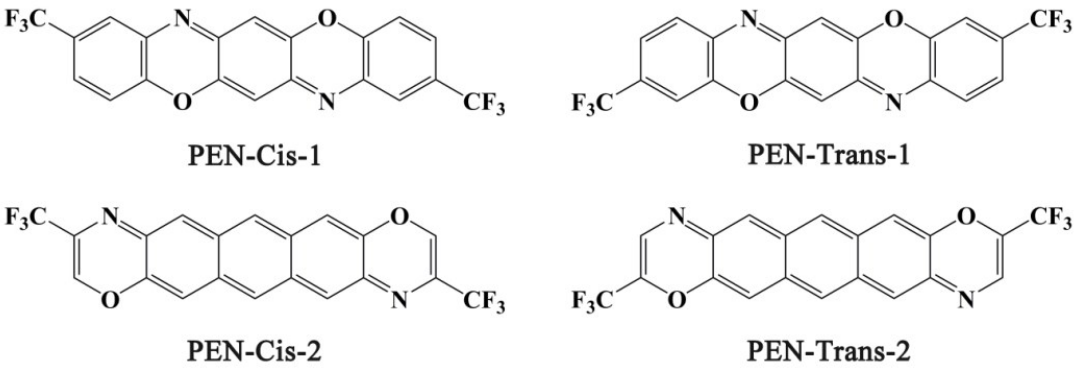

Fig. S2 The chemical structure of the derivatives of PEN.

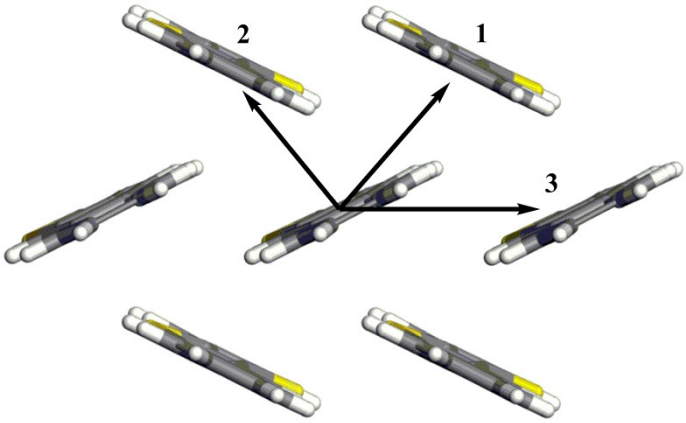

Fig. S3 The packing of **DNTT**.

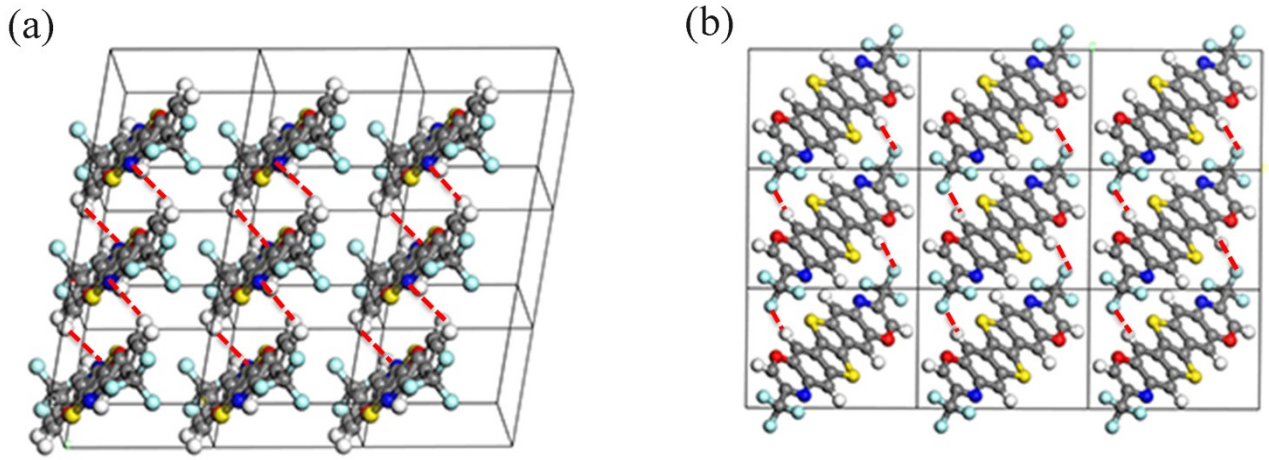

Fig. S4. The networks of hydrogen bond for crystal packing for ***Cis***-isomers: (a) is ***Cis-1*** and the red dotted line represented C-H···N ($d_{H\cdots N}$=2.647 Å) hydrogen bonding. (b) is ***Cis-2*** and the red dotted line represented C-H···F hydrogen bonding ($d_{H\cdots F}$=2.725 Å).

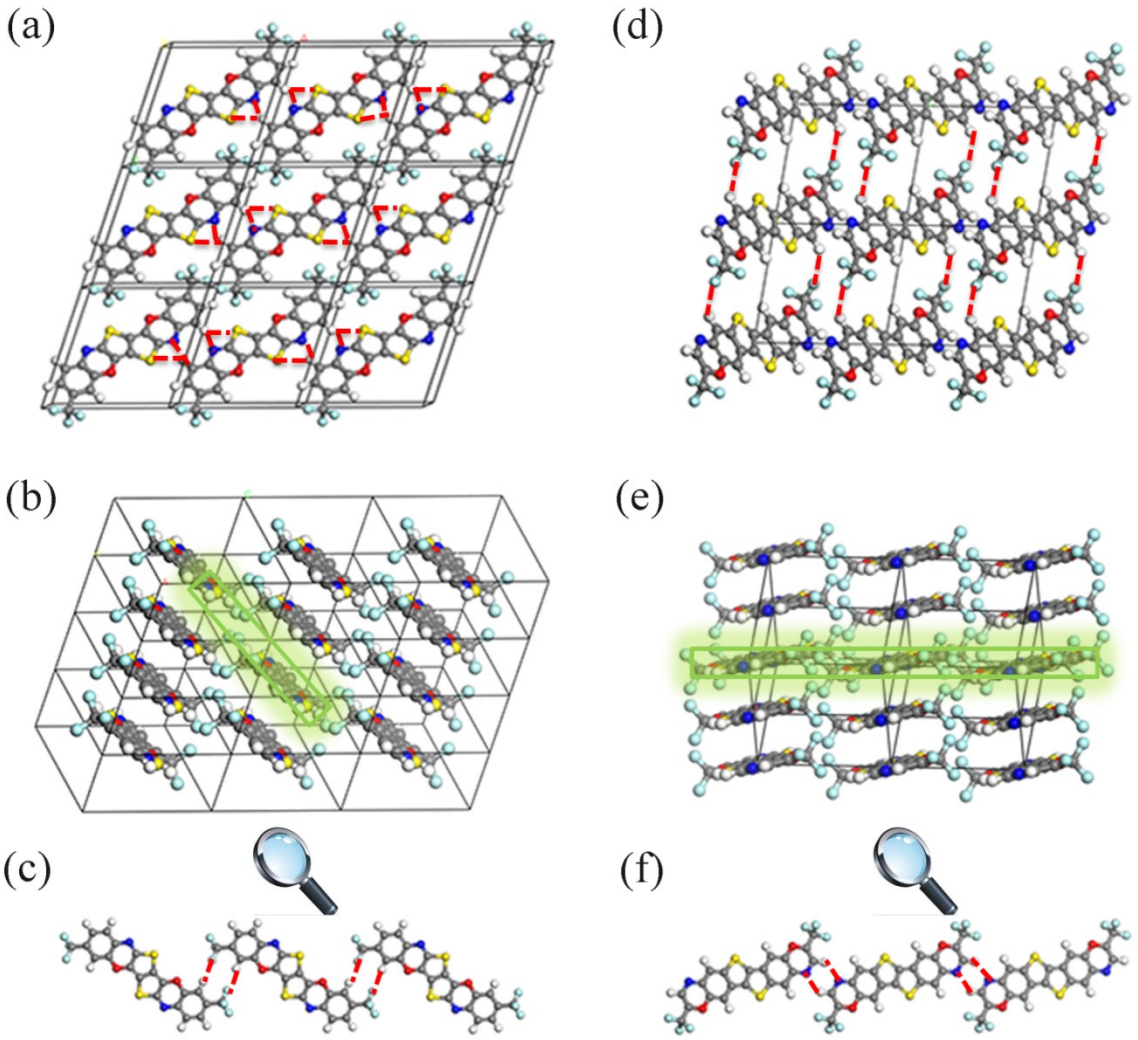

Fig. S5. The networks of hydrogen bond for crystal packing for ***Trans***-isomers: (a) ~ (c) are ***Trans-1***, the red dotted line represented C-H···N and C-H···S hydrogen bonding in (a); $d_{H\cdots N}$=2.727 Å, and $d_{H\cdots S}$=2.875 Å. C-H···F hydrogen bonding in (b) and (c), $d_{H\cdots F}$=2.392 Å. (d) ~ (f) are ***Trans-2***, the red dotted line represented C-H···F hydrogen bonding in (d) and $d_{H\cdots F}$=2.304 Å; C-H···N hydrogen bonding in (e) and (f), $d_{H\cdots N}$=2.289 Å.

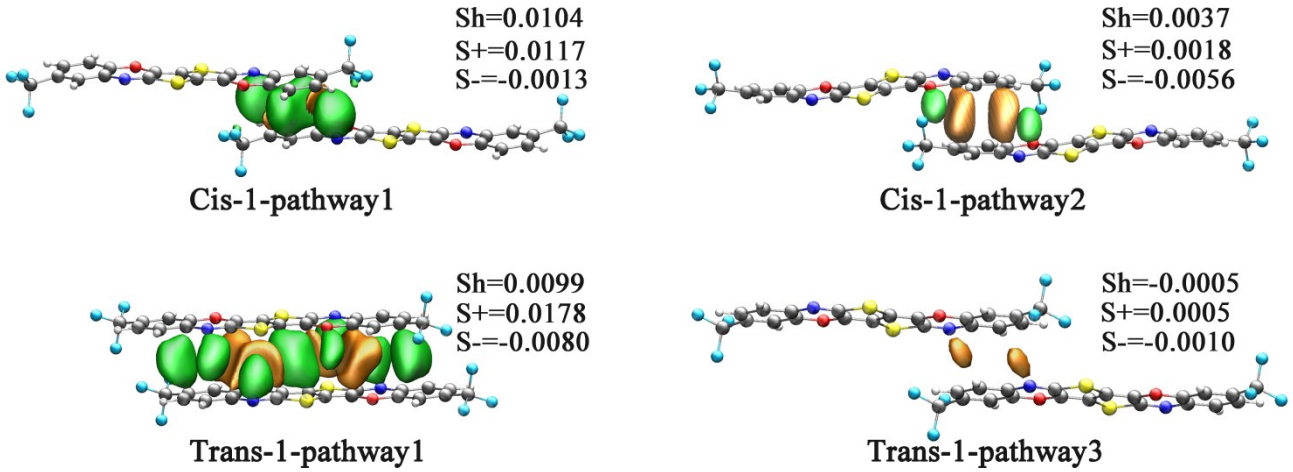

Fig. S6 The HOMO orbital overlap integral of ***Cis-1*** and ***Trans-1*** molecules, green represents in-phase overlap and orange represents in reverse phase overlap; Sh is the total overlap integral values of HOMO, which is the sum of in-phase overlap integral value (S+) and in reverse phase overlap integral value (S-).

Clearly, for ***Cis-1***, the symmetry of HOMO orbital for pathway1 is well matched and its orbital overlap integral value is as high as 0.0104. Compared with pathway1, the symmetry matching of HOMO orbital for pathway2 is slight poor. For ***Trans-1***, although the small slip distance along the molecular both long- and short-axis of pathway1, leads to the conjugate rings are dislocated from each other, furthermore, the symmetry of HOMO orbital matched relatively poor. Since the large slip distance along the molecular long- and short-axis of pathway2, the orbital symmetry matching is poor.

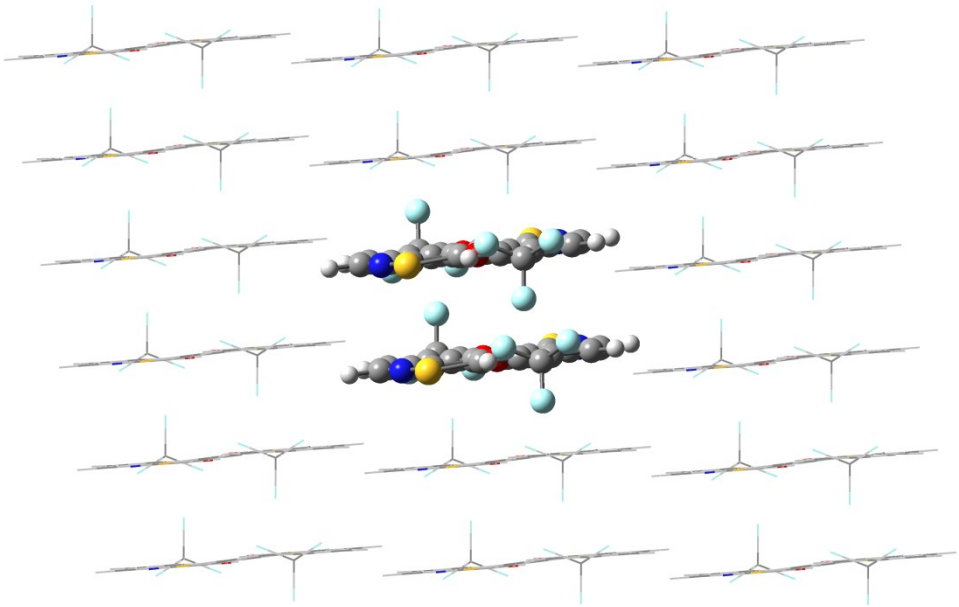

Fig. S7. The center dimer displayed with ball and stick model represents the region optimized by QM; and the surrounding molecules displayed with wire model represent the region treated with MM.

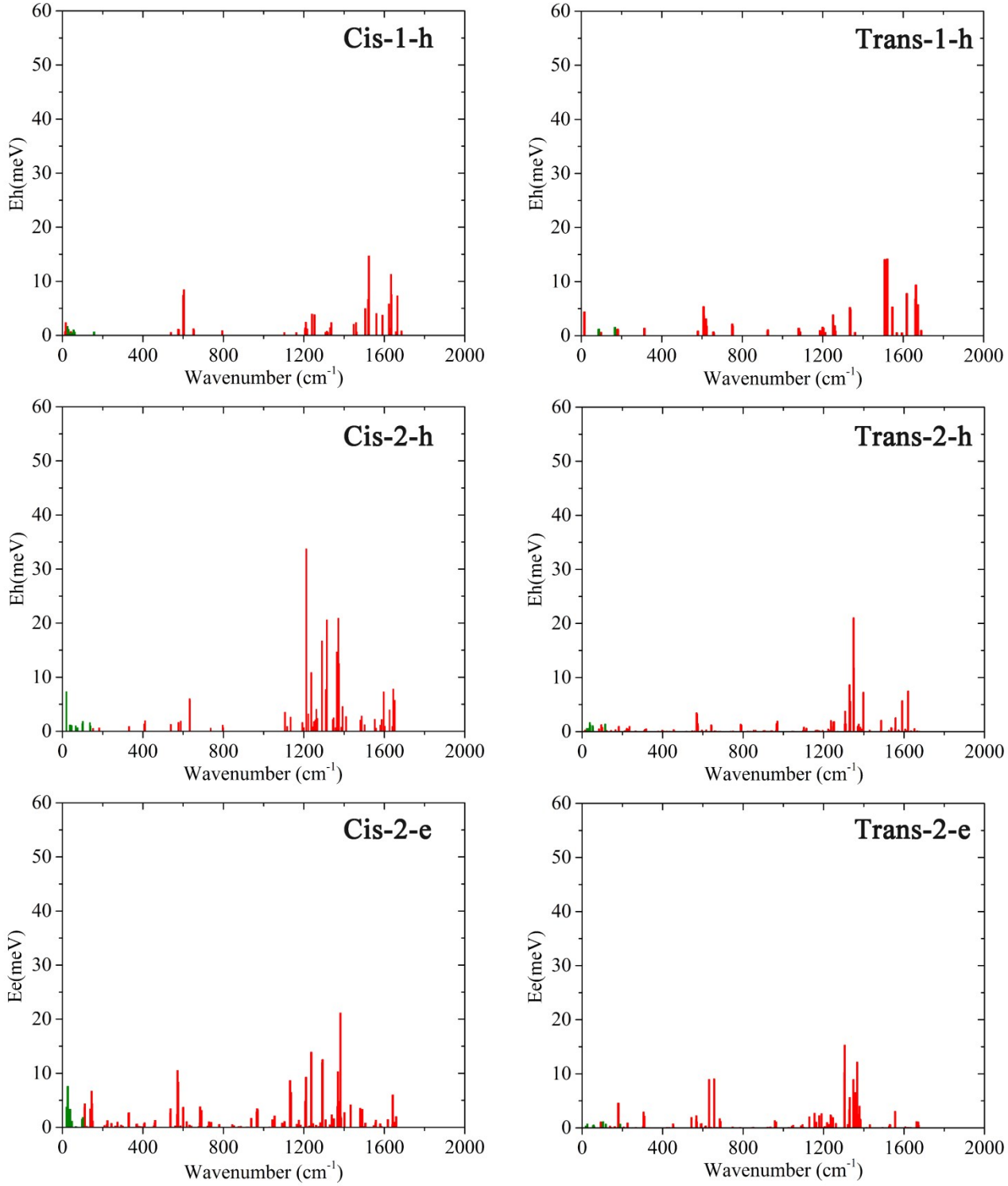

Fig. S8. The vibrational modes (green represents intermolecular and red represents intramolecular) contributing to nonlocal electron-phonon coupling.

In order to find out the specific phonon modes that contribute most to the electron-phonon coupling and thermal disorder, we use the quantum mechanics and molecular mechanics (QM/MM) approach in Gaussian 09 program ONIOM module to calculate the contributions of dimer's vibration

modes to the electron-phonon coupling. In the QM/MM model, the nearest dimer is selected as the high layer and it was calculated by the quantum mechanical method at the B3LYP/6-31G(d, p) level, while the surrounding molecules were served as the low layer calculated by molecular mechanics with the Universal Force Field (UFF). In addition, the "frozen optimization" method was used to obtain the frequency, which means that the optimization only occurs in the central dimer, while other surrounding molecules are frozen. The contributions of each vibration mode of single molecule in the gas phase to reorganization energy are shown in **Fig 2**. By comparing **Fig. 2** with **Fig. S8**, some vibration modes that contribute to the relaxation energy are found in the low frequency region of **Fig. S8**. These vibration modes are caused by intermolecular vibration. Then, we listed these intermolecular vibration modes in **Fig. 7** to analysis the effect of intermolecular vibration on thermal disorder.

The Comparison between *DNTT* Derivatives and *PEN* Derivatives

Here, we also calculated the single-molecule properties of ***PEN*** derivatives. The molecular structures were shown in **Fig. S2** and the calculated results were listed in **Table 2**. In comparison with ***PEN*** derivatives, the four ***DNTT*** derivatives have slightly smaller λ_h, and some ***DNTT*** derivatives (heteroatom in the terminal benzene ring) have slightly smaller λ_e, while others (heteroatom in the central benzene ring) have larger λ_e. Next, comparing the HOMO and LUMO levels of ***PEN*** and ***DNTT*** derivatives, we can see that the trend of the FMO levels of their derivatives is the same, that is, the HOMO and LUMO levels are almost independent on the position of $-CF_3$ and dependent on the position of O- and N-atoms. Compared with ***PEN*** derivatives, ***DNTT*** derivatives (heteroatom in the central benzene ring) have higher HOMO and slightly higher LUMO. Showing that there is little difference in electron injection, but some difference in hole injection (***DNTT*** derivatives are more favorable than ***PEN*** derivatives). Considering the λ and FMO energy levels, when incorporate O- and N-atoms into the central benzene ring, ***PEN*** derivatives are n-channel candidates and ***DNTT*** derivatives are p-channel candidates; when incorporate O- and N-atoms into the terminal benzene ring, ***PEN*** and ***DNTT*** derivatives are ambipolar candidates, but the carrier transport properties of ***PEN*** derivatives are not better than those of ***DNTT*** derivatives.

Table S1 The calculated hole and electron reorganization energy (λ_h/λ_e, in meV), HOMO and LUMO level energies (in eV, the experiment values of HOMO and LUMO of PEN-Cis-1 and PEN-Trans-1[1] are also listed), adiabatic ionization potentials and electron affinities (AIP/AEA, in eV) for PEN derivatives.

	λ_h(AP)	λ_e(AP)	HOMO	LUMO	AIP	AEA
PEN	93	132	-4.88	-2.69	5.90	1.14
PEN-Cis-1	290	362	-6.03/-6.04^{exp}	-3.53/-3.67^{exp}	7.21	2.40
PEN-Trans-1	271	395	-6.05/-6.06^{exp}	-3.60/-3.67^{exp}	7.24	2.49
PEN-Cis-2	229	268	-5.53	-4.00	6.69	2.89
PEN-Trans-2	228	338	-5.56	-4.11	6.71	3.06

1. C. A. Di, J. Li, G. Yu, Y. Xiao, Y. Guo, Y. Liu, X. Qian and D. Zhu, *Org. Lett.*, 2008, **10**, 3025-3028.